



Adverse Effects of Increasing Drought on Air Quality via Natural Processes

Yuxuan Wang^{1,2*}, Yuanyu Xie^{1*}, Wenhao Dong¹, Yi Ming³, Jun Wang⁴, Lu Shen⁵

¹Department of Earth System Sciences, Tsinghua University, Beijing, China

5 ²Department of Earth and Atmospheric Sciences, University of Houston, Houston, TX, USA

³NOAA/Geophysical Fluid Dynamics Laboratory, Princeton, NJ, USA

⁴Center for Global and Regional Environmental Research & Dept. of Chemical and Biochemical Engineering & Interdisciplinary Graduate Program in GeoInformatics, University of Iowa, Iowa City, IA, USA

10 ⁵School of Engineering and Applied Science, Harvard University, Cambridge, MA, USA

*These authors contributed equally to this work.

Correspondence to: ywang246@central.uh.edu; xiyy12@mails.tsinghua.edu.cn

Abstract. Drought is a recurring extreme of the climate system with well-documented impacts on agriculture and water resources. The strong perturbation of drought to the land biosphere and atmospheric water cycle will affect atmospheric composition, the nature and extent of which are not well understood. Here we present observational evidence that surface ozone and PM_{2.5} in the US are significantly correlated with drought severity, with 3.5 ppbv (8%) and 1.6 $\mu\text{g m}^{-3}$ (17%) increases respectively under severe drought. These enhancements show little sensitivity to the decreasing trend of US anthropogenic emissions, indicating natural processes as the primary cause. Elevated ozone and PM_{2.5} are attributed to the combined effects of drought on natural emissions (wildfires, biogenic VOCs and dust), deposition, and chemistry. Most climate-chemistry models are not able to reproduce the observed responses of ozone and PM_{2.5} to drought severity, suggesting a lack of mechanistic understanding of drought effects on atmospheric composition. The model deficiencies are partly attributed to the lack of drought-induced changes in land-atmosphere exchanges of reactive gases and particles and misrepresentation of cloud changes under drought conditions. By applying the observed relationships between drought and air pollutants to climate model projected drought occurrences, we estimate an increase of 1-6% for ground-level O₃ and 1-16% for PM_{2.5} in the US by 2100 compared to the 2000s due to increasing drought alone. Drought thus poses another aspect of climate change penalty on air quality not recognized before. Improvements in the models are imperative to facilitate better prediction of air quality challenges due to changing hydroclimate and atmospheric composition feedback to climate.

15
20
25



1. Introduction

Air pollution is a major global health risk (Forouzanfar et al., 2015). Chronic and acute exposure to enhanced ozone (O_3) and fine particulate matters with diameters less than $2.5 \mu m$ ($PM_{2.5}$) has been associated with many adverse health impacts and premature mortality (Lelieveld et al., 2015). Ambient O_3 and $PM_{2.5}$ concentrations are strongly regulated not only by atmosphere but also by land-atmosphere interactions through emission and deposition processes. To date, the variation of air quality with climate change has not been fully revealed as most analysis in the past were conducted with respect to atmospheric parameters or events only, such as temperature (Steiner et al., 2010), precipitation (Dawson et al., 2007; Allen et al., 2015), and short-term (in the order of days) meteorological anomalies (e.g., heat/cold waves, air stagnation, and temperature inversion) (Filleul et al., 2006; Qu et al., 2015; Hou and Wu, 2016). The impact of changing hydroclimate on air pollution is largely unexplored and highly uncertain, particularly with respects to droughts, a type of complex extremes recurring in many parts of the world that could affect atmosphere, land, and their interactions from weeks to seasons and even years.

Drought is characterized by a prolonged period of precipitation shortage and soil moisture deficit in combination with high temperatures (Trenberth et al., 2014). Besides significant impacts on agriculture and water resources (Rosenzweig et al., 2001; Arnell, 2004), drought conditions affect precipitation scavenging, chemical production/loss, and hence atmospheric lifetime of atmospheric constituents (Wang et al., 2015). Through changing the health and conditions of soil and vegetation cover across the landscape, drought can perturb upward transmission of dusts (Prospero and Lamb, 2003) and reactive gases (e.g., biogenic volatile organic compounds or BVOCs and NO_x) (Fuentes et al., 2000; Guenther et al., 2012; Guenther, 2015; Davidson et al., 2008) from the surface into the atmosphere as well as downward dry deposition of gases and aerosols (Huang et al., 2016). Complications such as increasing wildfires and changing human activities (Westerling et al., 2003; Scanlon et al., 2013) further compound the effects of drought on atmospheric composition. Climate change has the potential to increase the frequency and magnitude of droughts in many parts of the world (Dai, 2012; Cook et al., 2015), underscoring the importance of understanding the full extent of drought impacts. In this study we first quantify the impact of historical droughts on air quality, an area largely overlooked in prior investigations of drought impacts, and discuss the possible causes of those impacts. We then assess the performance of current chemistry-climate models in capturing the response of surface air pollutants to drought. Future changes in air quality related to increasing drought are estimated.

2. Data and Method

2.1 Drought index

Among many types of drought indicators, we chose the standardized precipitation evapotranspiration index (Vicente-Serrano et al., 2010) (SPEI) because it is multiscalar in representing the drought duration and its formulation explicitly considers the impact of temperature variability on water balance. The gridded SPEI datasets are obtained from the global SPEI database (<http://sac.csic.es/spei/>) with a spatial resolution of $0.5^\circ \times 0.5^\circ$. The study period is 1990-2014 and the regional focus is the continental US where observational records of atmospheric composition are most abundant. We focus on the growth season (March-October) during which drought has most deleterious impacts on the land and biosphere. To identify the full extent of drought impacts and differentiate drought from normal variability in the hydrological cycle, we used the 1-month SPEI to select droughts lasting more than one month. Negative SPEI indicates drought. A more strict criteria of $SPEI < -1.3$ (the lowest 10th percentile of SPEI) was used here to distinguish drought conditions from non-drought conditions (SPEI between -0.5 to 0.5). To test the robustness of the drought-pollution relationship derived from SPEI, we used the Palmer Drought Severity Index (PDSI) to evaluate this relationship. The PDSI is the most widely used index of meteorological drought in the US and best represents long-term drought (~12 months) (Heim et al., 2002). Among all forms of PDSI, sc_PDSI_pm is the most updated version with self-calibration and improved formulation of calculating potential evapotranspiration (Dai, 2011). The sc_PDSI_pm dataset is monthly with a spatial resolution of $2.5^\circ \times 2.5^\circ$ (Assessed from <http://www.cgd.ucar.edu/cas/catalog/climind/pdsi.html>). Drought conditions were identified when $sc_PDSI_pm < -3$.

Figure 1a shows the percent occurrence of drought months ($SPEI < -1.3$) over the continental US during the study period. The Western US, Great Plains, Southeast US and southern part of the Northeast US clearly stand out as the most drought prone



regions, with extreme droughts occurring 10%-25% of time, ranging between 20 and 40 months during the past 25 years (Figure 1b). Recent examples of infamous droughts are the 2011 Texas drought (Nielsen-Gammon, 2012), the 2012 Great Plains drought (Hoerling et al., 2014), and the 2014-2015 California drought (Griffin and Anchukaitis, 2014). The PDSI-derived drought occurrence frequency ($sc_PDSI_pm < -3$; Figure S1) shows a similar pattern. However, the areas with more than 10% drought occurrence based on sc_PDSI_pm are much smaller than those based on SPEI (Figure S1a). This is partly because the two indices represent drought at different time scales (i.e. one month for SPEI versus 12 months for sc_PDSI_pm).

2.2 Air pollution and meteorological data

Surface concentrations of $PM_{2.5}$ and maximum daily 8 hour running average (MDA8) ozone over the same period were derived from daily observations collected over more than 2000 surface sites from the US Environmental Protection Agency Air Quality System (EPA-AQS) (http://aqsdrl.epa.gov/aqsweb/aqstmp/airdata/download_files.html), Clean Air Status and Trends Network (CASNET; <https://www.epa.gov/castnet>), and the Interagency Monitoring of Protected Visual Environments (IMPROVE) (Malm et al., 1994, <http://views.cira.colostate.edu/>) networks. Those daily observations were averaged to monthly means for analysis. The site-specific SPEI is the SPEI at the grid containing each site. Speciated $PM_{2.5}$ data was obtained from the Speciation Trend Networks (STN), which is a subset of the EPA AQS with about 180 sites. Sulfate wet depositions were collected from the National Atmospheric Deposition Program (NADP; <http://nadp.isws.illinois.edu/>). Isoprene concentrations were obtained from the Photochemical Assessment Monitoring Stations (PAMS) network (<https://www3.epa.gov/ttnamti1/pamsdata.html>). Surface data at each site was deseasonalized and detrended by removing the 7-year moving averages from the raw data time series for each month to derive the anomalies (c.f. Figure S2 for an example of data processing). The relationship between SPEI and air pollution anomalies was calculated by linear regression, and the p values are obtained from two-tailed F -test. Regional analysis focuses on four geographical divisions of the continental US (Figure 1a): the Western US [128°W-106°W, 30°N-50°N], the Great Plains [106°W-96°W, 25°N-50°N], the Southeast US [96°W-75°W, 25°N-38°N] and the Northeast US [96°W-63°W, 38°N-50°N].

Fire emissions were obtained from the Global Fire Emission Database (GFED) at a $0.25^\circ \times 0.25^\circ$ resolution (Giglio et al., 2013; Randerson et al., 2012; Van der Werf et al., 2010; Akagi et al., 2011; <http://www.falw.vu/~gwerf/GFED/GFED4/>). The spatial impacts of fire smokes can range from a few kilometers to thousands of kilometers depending on the burning area/intensity, injection height, and transport conditions. Fire emissions from 9 grid points (~40 km) around each surface site were sampled to represent the immediate and transported impacts of fires. Temperature, precipitation, incoming shortwave radiation, and cloud fraction were obtained from the Modern Era Retrospective Analysis for Research and Applications (MERRA) reanalysis (Rienecker et al., 2011) (<http://giovanni.gsfc.nasa.gov/giovanni/>). Monthly mean cloud fractions below 680 hPa from satellite observations were obtained from the Clouds and the Earth's Radiant Energy System (CERES) ISCCP-D2like products at a spatial resolution of $1^\circ \times 1^\circ$ for the period of 2000 to 2014 (Minnis et al., 2011, https://eosweb.larc.nasa.gov/project/ceres/isccp-d2like-merged_ed3a_table). The site-specific meteorological parameters were retrieved from the grid that contains a surface site.

2.3 Models

We evaluated the SPEI-pollution relationships simulated by four models from the Atmospheric Chemistry and Climate Model Intercomparison Project (ACCMIP) (Lamarque et al., 2013) that have archived ozone and $PM_{2.5}$ concentrations: GISS-E2-R, GFDL-AM3, NCAR-CAM3.5, and MIROC-CHEM (Downloaded from <http://browse.ceda.ac.uk/>). The ACCMIP experiments were forced with observed greenhouse gases concentrations from historical runs. The four models used the same anthropogenic and biomass burning emissions of ozone and aerosol precursors (Lamarque et al., 2010). While anthropogenic emissions were yearly specific, biomass burning emissions were present at the decadal mean without inter-annual variations within a specific decade. The treatment of natural emissions varies between models, depending on meteorological and surface conditions. The GISS-E2-R model simulates isoprene emissions as coupled with its meteorology, while the GFDL-AM3, NCAR-CAM3.5 and MIROC-CHEM model used prescribed emissions. ACCMIP focuses on time-sliced experiments, thus each model covers different time periods. Model ozone and $PM_{2.5}$ were deseasonalized and detrended for each time slice



experiment in order to remove the effect of changes in anthropogenic emissions. The model SPEI was calculated using the R package based on simulated precipitation and temperature from each model. The relationship of SPEI with air pollution anomalies was derived over all the time periods with available model outputs. To evaluate low-altitude cloud fractions in the model, which is most relevant to atmospheric chemistry, we calculated the cloud fraction below 680 hPa using the random overlap (Stephens et al., 2004). Further details on the model experiments and data processing are listed in Supplementary Table 1.

3. Retrospective Analysis

3.1 Effects of drought on air pollutants

We first derived the general association of surface ozone and $PM_{2.5}$ with the SPEI at the surface sites (Figure 1). Concentrations at each surface site were deseasonalized and detrended (as described in Section 2.2) to remove the effects of seasonality and long-term changes in anthropogenic emissions, and the resulting anomalies were used for analysis. Ozone and $PM_{2.5}$ anomalies show statistically significant and spatially prevalent negative correlations with SPEI (Figure S3) at 75% - 88% of the sites. The slopes from linear regression suggest larger sensitivities to drought for both ozone (-2.63) and $PM_{2.5}$ (-1.0) in the east (Figure 1c, e). These slopes indicate that decreasing SPEI by one standard deviation will lead to an average increase of 2.21 (± 0.85) ppbv for ozone and 0.83 (± 0.37) $\mu\text{g m}^{-3}$ for $PM_{2.5}$ in the US. The slope from linear correlation between sc_PDSI_pm and ozone and $PM_{2.5}$ are shown in Figure S1. There are 52-74% sites showing negative correlations, a lower percentage compared to the correlations based on SPEI because SPEI has more accurate representation of drought at the monthly scale than sc_PDSI_pm .

To further distinguish the drought effects, we aggregated pollutant anomalies from the sites with greater than 10% occurrence of drought onto three dryness levels: drought (SPEI < -1.3), normal (SPEI between -0.5 and 0.5), and wet (SPEI > -1.3). This composite comparison reveals significantly higher levels of both pollutants during drought as compared to normal and wet conditions, which is evident consistently across all the regions (Fig. 1d, f). Average enhancement in the US is 3.5 (6.6) ppbv for ozone and 1.6 (2.5) $\mu\text{g m}^{-3}$ for $PM_{2.5}$ under drought as compared to normal (wet) conditions. The eastern sites show a larger increase of ozone at 3.9 (7.3) ppbv and $PM_{2.5}$ at 2.0 (3.1) $\mu\text{g m}^{-3}$ under drought as compared to normal (wet) conditions, consistent with the spatial distribution of the regression slopes. The relative change is similar across regions at about 8% (16%) for ozone and 17% (31%) for $PM_{2.5}$ (Figure S4).

The distribution of ozone and $PM_{2.5}$ anomalies at different dryness levels based on sc_PDSI_pm are displayed in Figure S1 (d and f). Since drought frequency represented by sc_PDSI_pm is comparatively lower, we chose sites with more than 5% drought occurrence based on sc_PDSI_pm and 5 years of available surface observations to reduce the spatial sampling bias. Compared to normal (wet) conditions, the average enhancement during drought is 4.7 (7.9) ppb for O_3 and 2.4 (3.0) $\mu\text{g m}^{-3}$ for $PM_{2.5}$ over the eastern sites. The relative change is consistent across different regions at about 7% for ozone and 18% for $PM_{2.5}$. The negative correlations as well as ozone/ $PM_{2.5}$ enhancements under drought conditions using sc_PDSI_pm are similar to those derived with SPEI, thus validating the robustness of the response of ozone/ $PM_{2.5}$ under drought conditions and suggesting little sensitivity of our analysis to the choice of drought indicator.

3.2 Causes of ozone and $PM_{2.5}$ enhancement by drought

Drought can affect air quality through perturbations to emissions, chemical processes and deposition. The ozone enhancement due to drought is primarily associated with higher temperatures (1.1°C - 2.0 °C) and stronger shortwave radiation (8.1-12.4 W m^{-2}) (Table S2). These conditions lead to higher production rate of ozone as well as higher emissions of BVOCs (Fuentes et al., 2000; Guenther et al., 2012). Surface observations of isoprene suggest 7-20% higher concentrations under drought conditions (Table 1). A decrease in isoprene is found during severe drought (SPEI < -2) over the southeast and northeast US (Figure 2), presumably due to shutoff of isoprene emissions when severe water stress causes reduction in carbon sources, lower level of isoprene synthase gene expression, stomata closure and wilting of vegetation (Pegoraro et al., 2004; Brilli et al., 2007; Seco et al., 2015). Surface NO_2 was also found to be 0.07-1.26 ppb (2-9%) higher, attributable to increased emissions from fires, soils



and possibly the power sector. In addition, ozone dry deposition can be reduced by up to 20% due to lower stomatal conductance under drought (Huang et al., 2016).

Changes in PM_{2.5} species, presented in Figure 3 at a subset of surface sites with speciation measurements, indicate that organic aerosol (OA), sulfate and dust are major contributors to the overall PM_{2.5} enhancements. Wet deposition of inorganic species measured by the National Atmospheric Deposition Program suggest a 23-32% reduction in sulfate wet deposition during drought (Table 1), explaining partly the 2-15% sulfate increase. While oxidation rate of SO₂ may increase at high temperatures (Tai et al., 2010), there is a 1-10% increase in surface SO₂ during drought resulting from reduced dry or wet deposition and higher emissions from fires and electricity generation (Scanlon et al., 2013). Dust enhancement is most significant in the west (27%) and the Great Plains (16%) due to more semi-arid areas. Drought causes significant OA enhancements (12-35%) across all the US. Fire emissions of primary OA are 1-3 times higher during drought, explaining a large portion of the OA enhancement (Tables S3-4). When excluding the fire influences, an increase in the OA to BC ratio was found under drought (Figure S5), suggesting an increase in secondary organic aerosols (SOA) formation. However, routine networks provide only limited classification of OA and cannot fully distinguish the response of SOA to drought from that of total OA.

Changes in ozone and PM_{2.5} are largely responses of natural processes from the land biosphere and abnormal atmospheric conditions. To compare the drought-induced changes with the effects of anthropogenic emission reductions in the US, we divided the data into two sub-periods: 1990 to 2003 (P1) and 2004 to 2014 (P2). Anthropogenic emissions of PM_{2.5} and ozone precursors have decreased significantly in the US from P1 to P2, for example, by 50% for SO₂ and 32% for NO_x according to the Air Pollutant Emission Trend Data from the US EPA (EPA, 2016). In spite of this, drought-induced enhancements of pollutants are manifested clearly in observational data for both periods and the magnitude of these enhancements remains the same between P1 and P2 (Table 2). Under normal conditions, the decrease of ozone (1.6 ppbv) and PM_{2.5} (1.8 µg m⁻³) from P1 to P2 is attributable to the reductions of US anthropogenic emissions. By comparison, drought-induced enhancement of ozone exceeds 4 ppbv in both periods and that of PM_{2.5} is 1.6 µg m⁻³. This demonstrates the significantly adverse impact of increasing drought on air quality through natural processes, which offset the benefits of reductions in anthropogenic emissions.

3.3 Modeled response of air pollutants to drought

Previous studies suggest that climate models have some skills to predict the variability of drought (Dai, 2012). Indeed the four models from ACCMIP all successfully reproduce the observed statistics of historical droughts in the US (Figure S6). In spite of this, the models vary greatly in their ability of predicting the effects of drought on atmospheric composition. With respects to surface ozone, all the models are able to capture its negative correlation with SPEI over most of the US (Figure 4), as they all predict some levels of increase in ozone production driven by higher temperatures during drought (Figure S7). However, the simulated slopes and magnitude of ozone enhancement are less than half of the observed values in many regions, suggesting a lack of full representation of the drought effects, especially on natural emissions and dry deposition through drought perturbation of the land biosphere. The GISS-E2-R model, which has BVOCs emissions coupled with weather/climate, reproduces the observed isoprene increases and thus simulates relatively larger ozone enhancement under drought conditions (Figure S7). The MICRO-CHEM model shows higher ozone enhancements than other models because it simulates the largest increase of ozone production caused by drought, presumably due to a larger sensitivity of ozone to temperature. All the models simulate little changes of ozone dry deposition (-3~5%) during drought.

The models are less skillful in reproducing the effects of drought on PM_{2.5} (Figure 5). All the models incorrectly predict a decrease of PM_{2.5} under drought conditions and hence a positive PM_{2.5}-SPEI relationship for many regions in the US, whereas this relationship is clearly negative in the observations across all the regions. For the few regions where some models are correct about the direction of the PM_{2.5} change (e.g. the western US by GISS-E2-R and eastern US by NCAR-CAM3.5), the magnitude of the PM_{2.5} change is less than 70% of that observed. The model response is primarily driven by a ubiquitous and excessive decrease of sulfate under drought conditions caused by large reductions of sulfate production in clouds (-22~-73%) (Figure S8-9). In contrast, only 14-34% of the sites in the west and the Great Plains show a decrease of sulfate during drought. The model deficiency in sulfate can be explained by their underestimate of low-altitude cloud fraction at higher temperatures (Shen et al., 2016), which outweighs the deposition decrease. The simulated sensitivity of low-altitude cloud fraction to drought severity is 4.69 and 5.75 per unit increase of SPEI from the GISS and GFDL model respectively. By comparison,



satellite-derived low-altitude cloud fraction shows a sensitivity of only 0.52 per unit increase of SPEI (Figure 6). In addition, the models underestimate the OA enhancements for all the regions. OA changes in the model are primarily resulted from reduced wet deposition (~40%), lacking important contributions from changing BVOCs emissions, fires, or chemistry (Figure S8-9).

- 5 The model deficiencies suggest a lack of mechanistic understanding of drought effects on natural processes of importance to atmospheric composition. Specifically, the lack of biosphere responses and misrepresentation of cloud sensitivity to changing drought severity are the major contributors of the model deficiencies. While all the models simulate some levels of decreasing wet deposition, dry deposition in the model is largely insensitive to drought due to the lack of drought effects on the properties of the land and biosphere. Most models do not have the effects of drought on different types of natural emissions, e.g. from
10 fires, BVOCs, and dust.

4. Future changes in drought and adverse impacts on air quality

To circumvent the model deficiencies, the effects of future increases of drought on air quality were estimated by extrapolating their present-day relationships from observations to model projected drought occurrences under future warming scenarios. Projected changes in SPEI from the present to future climate were derived from the outputs of the four ACCMIP models (i.e.
15 GISS-E2-R, GFDL-CM3, CCSM4, and MIROC-ESM-CHEM) archived by the Coupled Model Intercomparison Project Phase 5 (CMIP5) (Taylor et al., 2012). The CMIP5 historical runs cover the period from 1850 to near present, and are forced with observed changes in atmospheric composition with evolving land cover. The future projection runs span from 2006 to 2300, forced with specified concentrations of certain atmospheric constituents defined in three representative concentration pathways (RCPs) scenarios (Moss et al., 2010): RCP 2.6 (low mitigation emission
20 scenario), RCP 4.5 (midrange mitigation emission scenario) and RCP 8.5 (high emission scenario). Changes in future drought conditions compared to the present are defined as the 2100 SPEI (2080-2099 mean) minus its value in 2000 (1990-2005 mean).

Figure 7a shows the projection of SPEI in the US by 2100 (2080-2099 mean) under different RCPs that are derived from the mean of the four models from the CMIP5 outputs. Drought risks are projected to increase with warming scenarios over all parts of the US, with the largest increases in the west and the Great Plains, consistent with previous projections (Cook et al., 2015).
25 These projected SPEI changes (2100 minus 2000), when multiplied by the present-day relationship between SPEI and air quality derived from observations (c.f. Figure 1), suggests a 0.3-3.0 ppb (1-6%) increase of surface ozone and 0.1-1.0 $\mu\text{g m}^{-3}$ (1-16%) increase of $\text{PM}_{2.5}$ in the US in 2100 as a result of increasing drought alone under different RCPs (Figure 7b-c). The increase of ozone and $\text{PM}_{2.5}$ are largest in the west. The maximum increase is 14% for ozone and 41% for $\text{PM}_{2.5}$ under the extreme warming scenario (RCP 8.5), significantly higher than the present-day effects. While this extrapolation-based
30 projection may not be reliable quantitatively, it suggests a significant climate change penalty on air quality through drought, which has been overlooked before and pose a new challenge for air quality managers.

5. Discussion

The retrospective analysis of observations demonstrates that past droughts have caused significant deterioration of air quality through natural processes, resulting in potentially large tolls on public health that have not been considered in previous impact
35 analysis of drought. The land biosphere plays a key role in mediating drought-induced changes in atmospheric chemistry. The magnitude of the land biosphere response is largely dependent on concurrent changes in solar irradiance, temperature and water at different levels of drought severity and duration. More sunlight and higher temperatures may outweigh some levels of water stress, resulting in enhanced BVOCs emissions through leaf biochemistry, vapor pressure difference and underlying metabolism processes (Fuentes et al., 2000). However, extreme and/or prolonged drought conditions with severe water stress
40 coupled with very high temperatures can affect the activity of enzyme and health of the plants, therefore leading to reductions in BVOCs emissions. More comprehensive understanding of the land biosphere responses is required to quantify the impact of land biosphere to atmospheric compositions under different drought conditions. In addition to changing BVOCs emissions, reduced aerosol water content under drought conditions can perturb aqueous phase formation of SOA from BVOCs, but the



5 impact is not clear (Gilarioni et al., 2016). Changes in anthropogenic emissions under drought conditions are also uncertain. Local land use type and water management policy can significantly affect human reactions to drought. Furthermore, the interaction between anthropogenic emissions and natural responses further compound the drought effect, as anthropogenic emitted gases and aerosols can affect the oxidation and partitioning processes of SOA from BVOCs (Hoyle et al., 2011; Xu et al., 2015).

10 Changes in the land biosphere and atmospheric compositions, including gases and aerosols, can provide feedbacks to the climate through radiative effects and cloud interactions. Reductions in vegetation cover affect surface albedo and dust emissions, resulting in enhanced surface temperatures, intensification of drought conditions and geographical shift of drought pattern (Cook et al., 2009). Increasing wildfire activity and fire-emitted aerosols alter the regional energy budget and circulation, which lead to reduced precipitation thus further enhancing drought severity and vulnerability of ecosystem towards wildfires (Bevan et al. 2009; Tosca et al., 2010; Hodnebrog et al., 2016). Improvements in climate-chemistry models are thus imperative to facilitate better prediction of atmospheric composition changes due to changes in drought and improved understanding of the associated feedbacks of composition changes to climate and drought itself.

15 The observational analysis presented here indicates significant changes of air pollutants under drought conditions. However, it is not sufficient to quantify the full extent of the cascading effects of drought on the complex chemistry of ozone and SOA, which would require more targeted measurements providing for example more classification of organic materials and modeling at the process level. Uncertainties exist in the model assessment since we are using a single version of simulation for each model and the study period is relatively short and may not represent the full simulation results. Nonetheless, both observations and model indicate the important role of the land biosphere and atmospheric conditions in regulating pollutant levels under drought conditions. Future air quality management should consider the adverse effects from increasing drought risks.



Data availability

All datasets used in this study are publically accessible.

Author contribution

- 5 Y. W. and Y. X. conceived the research idea. Y. X. and W.D. performed the analysis and Y. W. wrote the initial draft of the paper. All authors contributed to the interpretation of the results and the preparation of the manuscript.

Competing financial interests

The authors declare no competing financial interests.

10

Acknowledgements

- We thank the individuals and groups involved in making observations at IMPROVE, US EPA, CASNET, NADP and PAMS networks, and in preparing the SPEI, PDSI, GFED, MERRA and ISCCP-D2like database. We thank the modelling groups that participate in ACCMIP and CMIP5 for producing the model outputs and making them available. This work was supported in part by the National Key Basic Research Program of China (2013CB956603 and 2014CB441302). J. Wang acknowledges the support from NASA Aura Science program (grant #: NNX14AG01G managed by Dr. Ken Jucks), Applied Science Program (grant #: NNX15AC28A managed by Dr. John Haynes), and ACMAP program (grant #: NNX15AC30G managed by Dr. Richard Eckman).
- 15



References

- Akagi, S., Yokelson, R. J., Wiedinmyer, C., Alvarado, M., Reid, J., Karl, T., Crounse, J., and Wennberg, P.: Emission factors for open and domestic biomass burning for use in atmospheric models, *Atmospheric Chemistry and Physics*, 11, 4039-4072, 2011.
- 5 Allen, R. J., Landuyt, W., and Rumbold, S. T.: An increase in aerosol burden and radiative effects in a warmer world, *Nature Climate Change*, 6, 269-274, 10.1038/nclimate2827, 2015.
- Arnell, N. W.: Climate change and global water resources: SRES emissions and socio-economic scenarios, *Global environmental change*, 14, 31-52, 2004.
- Bevan, Suzanne L., et al.: Impact of atmospheric aerosol from biomass burning on Amazon dry - season drought. *Journal of Geophysical Research: Atmospheres* 114.D9, 2009.
- 10 Brill, F., Barta, C., Fortunati, A., Lerdau, M., Loreto, F., and Centritto, M.: Response of isoprene emission and carbon metabolism to drought in white poplar (*Populus alba*) saplings, *New Phytologist*, 175, 244-254, 2007.
- Cook, B. I., Miller, R. L., and Seager, R.: Amplification of the North American “Dust Bowl” drought through human-induced land degradation, *Proceedings of the National Academy of Sciences*, 106, 4997-5001, 2009.
- 15 Cook, B. I., Ault, T. R., and Smerdon, J. E.: Unprecedented 21st century drought risk in the American Southwest and Central Plains, *Science Advances*, 1, e1400082, 2015.
- Dai, A.: Characteristics and trends in various forms of the Palmer Drought Severity Index during 1900–2008, *Journal of Geophysical Research: Atmospheres*, 116, 2011.
- Dai, A.: Increasing drought under global warming in observations and models, *Nature Climate Change*, 3, 52-58, 10.1038/nclimate1633, 2012.
- 20 Davidson, E. A., Nepstad, D. C., Ishida, F. Y., and Brando, P. M.: Effects of an experimental drought and recovery on soil emissions of carbon dioxide, methane, nitrous oxide, and nitric oxide in a moist tropical forest, *Global Change Biology*, 14, 2582-2590, 2008.
- Dawson, J., Adams, P., and Pandis, S.: Sensitivity of PM 2.5 to climate in the Eastern US: a modeling case study, *Atmospheric Chemistry and Physics*, 7, 4295-4309, 2007.
- 25 Filleul, L., Cassadou, S., Mágina, S., Fabres, P., Lefranc, A., Eilstein, D., Le Tertre, A., Pascal, L., Chardon, B., Blanchard, M., Declercq, C., Jusot, J.-F., Prouvost, H., and Ledrans, M.: The Relation Between Temperature, Ozone, and Mortality in Nine French Cities During the Heat Wave of 2003, *Environmental health perspectives*, 114, 1344-1347, 10.1289/ehp.8328, 2006.
- 30 Forouzanfar, M. H., Alexander, L., Anderson, H. R., Bachman, V. F., Biryukov, S., Brauer, M., Burnett, R., Casey, D., Coates, M. M., and Cohen, A.: Global, regional, and national comparative risk assessment of 79 behavioural, environmental and occupational, and metabolic risks or clusters of risks in 188 countries, 1990–2013: a systematic analysis for the Global Burden of Disease Study 2013, *The Lancet*, 386, 2287-2323, 2015.
- 35 Fuentes, J. D., Gu, L., Lerdau, M., Atkinson, R., Baldocchi, D., Bottenheim, J., Ciccioli, P., Lamb, B., Geron, C., and Guenther, A.: Biogenic hydrocarbons in the atmospheric boundary layer: a review, *Bulletin of the American Meteorological Society*, 81, 1537-1575, 2000.
- Giglio, L., Randerson, J. T., and Werf, G. R.: Analysis of daily, monthly, and annual burned area using the fourth - generation global fire emissions database (GFED4), *Journal of Geophysical Research: Biogeosciences*, 118, 317-328, 2013.



- Gilardoni, S., Massoli, P., Paglione, M., Giulianelli, L., Carbone, C., Rinaldi, M., Decesari, S., Sandrini, S., Costabile, F., and Gobbi, G. P.: Direct observation of aqueous secondary organic aerosol from biomass-burning emissions, *Proceedings of the National Academy of Sciences*, 113, 10013-10018, 2016.
- Griffin, D., and Anchukaitis, K. J.: How unusual is the 2012–2014 California drought?, *Geophysical Research Letters*, 41, 9017-9023, 2014.
- 5 Guenther, A. B., et al.: The Model of Emissions of Gases and Aerosols from Nature version 2.1 (MEGAN2. 1): an extended and updated framework for modeling biogenic emissions. *Geoscientific Model Development*, 5.6: 1471-1492, 2012.
- Guenther, A. B.: Bidirectional exchange of volatile organic compounds. *Review and Integration of Biosphere-Atmosphere Modelling of Reactive Trace Gases and Volatile Aerosols*. Springer Netherlands, 107-113, 2015.
- 10 Heim Jr and Richard R.: A review of twentieth-century drought indices used in the United States. *Bulletin of the American Meteorological Society*, 83.8, 1149-1165, 2002.
- Hodnebrog, Ø., Myhre, G., Forster, P. M., Sillmann, J., and Samset, B. H.: Local biomass burning is a dominant cause of the observed precipitation reduction in southern Africa, *Nature communications*, 7, 2016.
- Hoerling, M., Eischeid, J., Kumar, A., Leung, R., Mariotti, A., Mo, K., Schubert, S., and Seager, R.: Causes and predictability of the 2012 Great Plains drought, *Bulletin of the American Meteorological Society*, 95, 269-282, 2014.
- 15 Hou, P., and Wu, S.: Long-term Changes in Extreme Air Pollution Meteorology and the Implications for Air Quality, *Scientific reports*, 6, 2016.
- Hoyle, C., Boy, M., Donahue, N., Fry, J., Glasius, M., Guenther, A., Hallar, A., Huff Hartz, K., Petters, M., and Petters, T.: A review of the anthropogenic influence on biogenic secondary organic aerosol, *Atmospheric Chemistry and Physics*, 11, 321-343, 2011.
- 20 Huang, L., McDonald-Buller, E. C., McGaughey, G., Kimura, Y., and Allen, D. T.: The impact of drought on ozone dry deposition over eastern Texas, *Atmospheric Environment*, 127, 176-186, 10.1016/j.atmosenv.2015.12.022, 2016.
- Lamarque, J.-F., Bond, T. C., Eyring, V., Granier, C., Heil, A., Klimont, Z., Lee, D., Liousse, C., Mieville, A., and Owen, B.: Historical (1850–2000) gridded anthropogenic and biomass burning emissions of reactive gases and aerosols: methodology and application, *Atmospheric Chemistry and Physics*, 10, 7017-7039, 2010.
- 25 Lamarque, J., Shindell, D. T., Josse, B., Young, P., Cionni, I., Eyring, V., Bergmann, D., Cameron-Smith, P., Collins, W. J., and Doherty, R.: The Atmospheric Chemistry and Climate Model Intercomparison Project (ACCMIP): overview and description of models, simulations and climate diagnostics, *Geoscientific Model Development*, 6, 179-206, 2013.
- Lelieveld, J., Evans, J. S., Fnais, M., Giannadaki, D., and Pozzer, A.: The contribution of outdoor air pollution sources to premature mortality on a global scale, *Nature*, 525, 367-371, 10.1038/nature15371, 2015.
- 30 Malm, W. C., Sisler, J. F., Huffman, D., Eldred, R. A., and Cahill, T. A.: Spatial and seasonal trends in particle concentration and optical extinction in the United States, *Journal of Geophysical Research: Atmospheres*, 99, 1347-1370, 1994.
- Minnis, Patrick, et al.: CERES edition-2 cloud property retrievals using TRMM VIRS and Terra and Aqua MODIS data—Part I: Algorithms. *IEEE Transactions on Geoscience and Remote Sensing* 49.11: 4374-4400, 2011.
- 35 Moss, R. H., Edmonds, J. A., Hibbard, K. A., Manning, M. R., Rose, S. K., Van Vuuren, D. P., Carter, T. R., Emori, S., Kainuma, M., and Kram, T.: The next generation of scenarios for climate change research and assessment, *Nature*, 463, 747-756, 2010.
- Nielsen-Gammon, J. W.: The 2011 Texas drought, *Texas Water Journal*, 3, 59-95, 2012.
- Pegoraro, E., Rey, A., Greenberg, J., Harley, P., Grace, J., Malhi, Y., and Guenther, A.: Effect of drought on isoprene emission rates from leaves of *Quercus virginiana* Mill, *Atmospheric Environment*, 38, 6149-6156, 2004.
- 40



- Prospero, J. M., and Lamb, P. J.: African droughts and dust transport to the Caribbean: Climate change implications, *Science*, 302, 1024-1027, 2003.
- Qu, W., Wang, J., Zhang, X., Yang, Z., and Gao, S.: Effect of cold wave on winter visibility over eastern China, *Journal of Geophysical Research: Atmospheres*, 120, 2394-2406, 2015.
- 5 Randerson, J., Chen, Y., Werf, G., Rogers, B., and Morton, D.: Global burned area and biomass burning emissions from small fires, *Journal of Geophysical Research: Biogeosciences*, 117, 2012.
- Rienecker, M. M., Suarez, M. J., Gelaro, R., Todling, R., Bacmeister, J., Liu, E., Bosilovich, M. G., Schubert, S. D., Takacs, L., and Kim, G.-K.: MERRA: NASA's modern-era retrospective analysis for research and applications, *Journal of Climate*, 24, 3624-3648, 2011.
- 10 Rosenzweig, C., Iglesias, A., Yang, X., Epstein, P. R., and Chivian, E.: Climate change and extreme weather events; implications for food production, plant diseases, and pests, *Global change & human health*, 2, 90-104, 2001.
- Seco, R., Karl, T., Guenther, A., Hosman, K.P., Pallardy, S.G., Gu, L., Geron, C., Harley, P. and Kim, S.: Ecosystem - scale volatile organic compound fluxes during an extreme drought in a broadleaf temperate forest of the Missouri Ozarks (central USA). *Global change biology*, 21.10: 3657-3674, 2015.
- 15 Scanlon, B. R., Duncan, I., and Reedy, R. C.: Drought and the water–energy nexus in Texas, *Environmental Research Letters*, 8, 045033, 2013.
- Shen, L., Mickley, L. J., and Murray, L. T.: Strong influence of 2000–2050 climate change on particulate matter in the United States: Results from a new statistical model, *Atmos. Chem. Phys. Discuss.*, doi:10.5194, 2016.
- Steiner, A. L., Davis, A. J., Sillman, S., Owen, R. C., Michalak, A. M., and Fiore, A. M.: Observed suppression of ozone formation at extremely high temperatures due to chemical and biophysical feedbacks, *Proceedings of the National Academy of Sciences*, 107, 19685-19690, 2010.
- Stephens, Graeme L., Norman B. Wood, and Philip M. Gabriel: An assessment of the parameterization of subgrid-scale cloud effects on radiative transfer. Part I: Vertical overlap. *Journal of the atmospheric sciences* 61.6: 715-732 2004.
- Tai, A. P. K., Mickley, L. J., and Jacob, D. J.: Correlations between fine particulate matter (PM_{2.5}) and meteorological variables in the United States: Implications for the sensitivity of PM_{2.5} to climate change, *Atmospheric Environment*, 44, 3976-3984, 10.1016/j.atmosenv.2010.06.060, 2010.
- 25 Taylor, K. E., Stouffer, R. J., and Meehl, G. A.: An overview of CMIP5 and the experiment design, *Bulletin of the American Meteorological Society*, 93, 485, 2012.
- Tosca, M., Randerson, J., Zender, C., Flanner, M., and Rasch, P. J.: Do biomass burning aerosols intensify drought in equatorial Asia during El Niño?, *Atmospheric Chemistry and Physics*, 10, 3515-3528, 2010.
- 30 Trenberth, K. E., Dai, A., van der Schrier, G., Jones, P. D., Barichivich, J., Briffa, K. R., and Sheffield, J.: Global warming and changes in drought, *Nature Climate Change*, 4, 17-22, 2014.
- U.S. Environmental Protection Agency: Technology Transfer Network Clearinghouse for Inventories and Emission Factors, National Emissions Inventory (NEI) air pollutant emissions trendsdata, 2016, <https://www.epa.gov/air-emissions-inventories/air-pollutant-emissions-trends-data> (last access: 10 Feb 2017).
- 35 Van der Werf, G. R., Randerson, J. T., Giglio, L., Collatz, G., Mu, M., Kasibhatla, P. S., Morton, D. C., DeFries, R., Jin, Y. v., and van Leeuwen, T. T.: Global fire emissions and the contribution of deforestation, savanna, forest, agricultural, and peat fires (1997–2009), *Atmospheric Chemistry and Physics*, 10, 11707-11735, 2010.
- Vicente-Serrano, S. M., Beguer á, S., and López-Moreno, J. I.: A Multiscalar Drought Index Sensitive to Global Warming: The Standardized Precipitation Evapotranspiration Index, *Journal of Climate*, 23, 1696-1718, 10.1175/2009jcli2909.1, 2010.
- 40



Wang, Y., Xie, Y., Cai, L., Dong, W., Zhang, Q., and Zhang, L.: Impact of the 2011 southern us drought on ground-level Fine aerosol concentration in summertime*, *Journal of the Atmospheric Sciences*, 72, 1075-1093, 2015.

Westerling, A. L., Gershunov, A., Brown, T. J., Cayan, D. R., and Dettinger, M. D.: Climate and wildfire in the western United States, *Bulletin of the American Meteorological Society*, 84, 595-604, 2003.

- 5 Xu, L., Guo, H., Boyd, C. M., Klein, M., Bougiatioti, A., Cerully, K. M., Hite, J. R., Isaacman-VanWertz, G., Kreisberg, N. M., and Knote, C.: Effects of anthropogenic emissions on aerosol formation from isoprene and monoterpenes in the southeastern United States, *Proceedings of the National Academy of Sciences*, 112, 37-42, 2015.

Tables

10 **Table 1: Changes in the concentrations of atmospheric gaseous compositions and sulfate wet deposition under drought compared to normal conditions. Data are from different measurement networks (see Method).**

		West	Great Plains	Southeast	Northeast
NO ₂ (ppb)	N ^a	130	27	81	122
	Diff	1.26 (+9.0%)	0.07 (+2.3%)	0.14 (+2.6%)	0.46 (+3.9%)
	p-value ^b	<0.01	0.68	0.25	<0.01
SO ₂ (ppb)	N	66	28	113	290
	Diff	0.14 (+2.6%)	0.13 (+1.4%)	0.29 (+10.4%)	0.32 (+7.3%)
	p-value	0.05	0.28	<0.01	<0.01
Isoprene (ppb carbon)	N	8	14	28	21
	Diff	0.21 (+11.6%)	0.01 (+7.0%)	0.09 (+13.8%)	0.36 (+19.5%)
	p-value	0.04	0.60	0.09	0.01
Sulfate wet deposition (kg month ⁻¹)	N	48	30	47	83
	Diff	-0.62 (-31.7%)	-1.39 (-26.7%)	-2.47 (-22.9%)	-2.99 (-26.2%)
	p-value	<0.01	<0.01	<0.01	<0.01

a. Number of sites.

b. P value derived from student t-test.



Table 2: Changes in the concentrations of ozone and PM_{2.5} at two periods under drought compared to normal conditions.

	P1 (1990-2003)			P2 (2004-2014)			P2 minus P1
	Drought	Normal	Diff	Drought	Normal	Diff	Normal
Ozone (ppbv)							
West	56.61	51.58	5.03	53.19	49.15	4.04	2.43
Great Plains	51.64	47.23	4.41	52.23	47.75	4.48	-0.52
Southeast	51.98	47.01	4.97	49.03	44.75	4.28	2.26
Northeast	51.64	46.43	5.21	48.19	44.23	3.96	2.20
Average	52.97	48.06	4.91	50.66	46.47	4.19	1.59
PM_{2.5} (µg m⁻³)							
West	6.57	5.56	1.01	5.84	4.74	1.10	0.82
Great Plains	7.69	6.22	1.47	6.86	5.81	1.05	0.41
Southeast	15.98	14.19	1.79	13.79	11.45	2.34	2.74
Northeast	16.37	14.25	2.12	12.67	10.94	1.73	3.31
Average	11.65	10.06	1.60	9.79	8.24	1.56	1.82



Figures

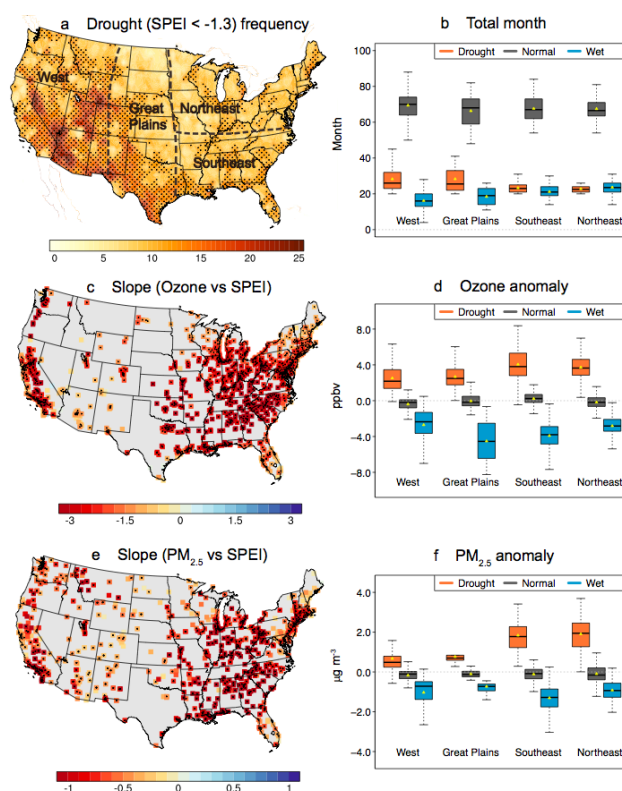


Figure 1: Percentage occurrence of severe drought months (SPEI < -1.3) over the continental US during 1990-2014 (a); black dots indicate drought frequency greater than 10% and dashed lines show the four geographical regions. Linear regression slope of SPEI with O₃ (c) and PM_{2.5} (e) anomalies at surface sites with data records longer than 5 years; yellow dots indicate regression significance at 95% confidence level. Boxplot comparisons of the number of months (b), ozone (d) and PM_{2.5} anomalies (f) under drought (SPEI < -1.3), normal (-0.5 < SPEI < 0.5) and wet conditions (SPEI > 1.3) by region; the yellow triangles in the boxplot indicate mean values. All the surface data shown in the boxplot are restricted to sites with data records longer than 5 years and more than 10% occurrence of severe drought (SPEI < -1.3).

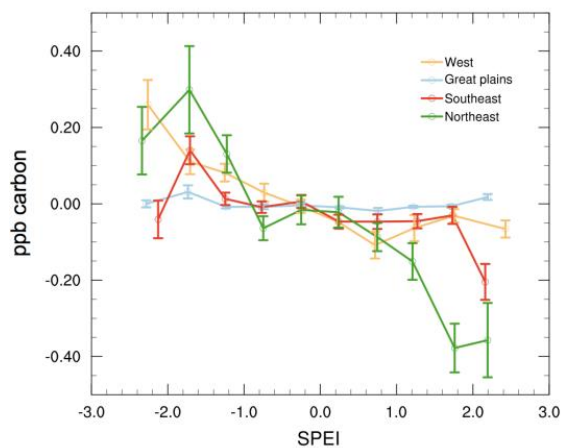
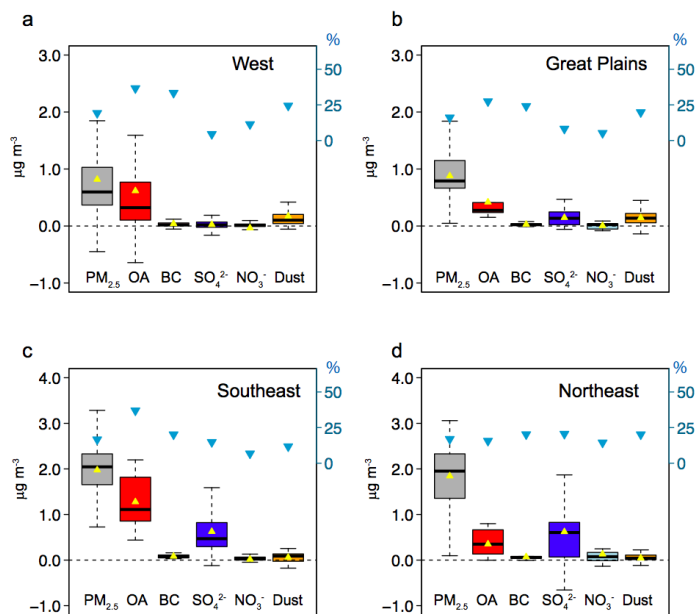


Figure 2: Isoprene anomalies (ppb carbon) derived from the PAMS network at binned SPEI levels over the Western, the Great Plains, the Southeastern and Northeastern US. Error bars indicate standard error of the mean.



5

Figure 3: Boxplot of anomalies in $PM_{2.5}$ speciation during drought ($SPEI < -1.3$) compared to normal ($-0.5 < SPEI < 0.5$) conditions for the Western (a), Great Plains (b), Southeastern (c) and Northeastern (d) US. The yellow triangle indicates mean values and blue triangles indicate relative changes (right y-axis).

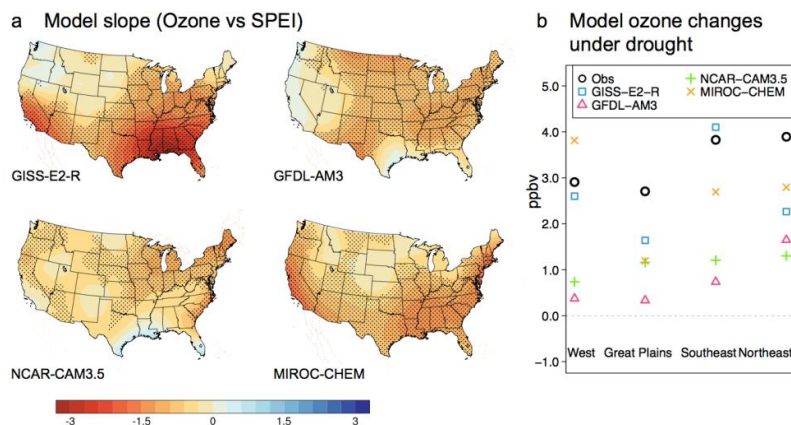


Figure 4: Linear regression slope between model derived SPEI and simulated ozone from GISS-E2-R, GFDL-AM3, NCAR-CAM3.5 and MIROC-CHEM model (a). Black dots represent regression significance at 95% confidence level. Note the color bar of (a) is the same as in Figure 1c. Comparison for the observed (black circle) and simulated changes (colored symbols) in ozone (b) under drought (SPEI < -1.3) compared to normal (-0.5 < SPEI < 0.5) condition by region.

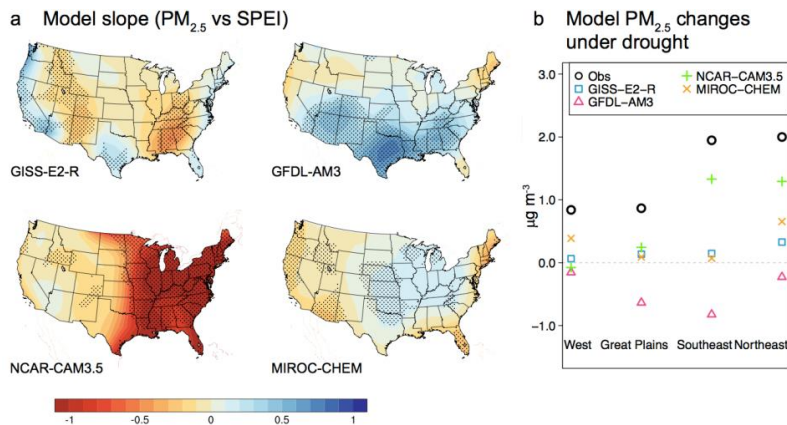


Figure 5: Linear regression slope between model derived SPEI and simulated PM_{2.5} from GISS-E2-R, GFDL-AM3, NCAR-CAM3.5 and MIROC-CHEM model (a). Black dots represent regression significance at 95% confidence level. Note the color bar of (a) is the same as in Figure 1e. Comparison for the observed (black circle) and simulated changes (colored symbols) in PM_{2.5} (b) under drought (SPEI < -1.3) compared to normal (-0.5 < SPEI < 0.5) condition by region.

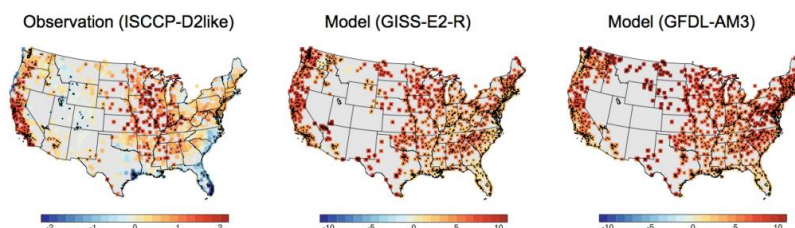


Figure 6: Slope from linear regression between SPEI and low cloud fractions from ISCCP satellite observations (left), GISS-E2-R (middle) and GFDL-AM3 model (right).

5

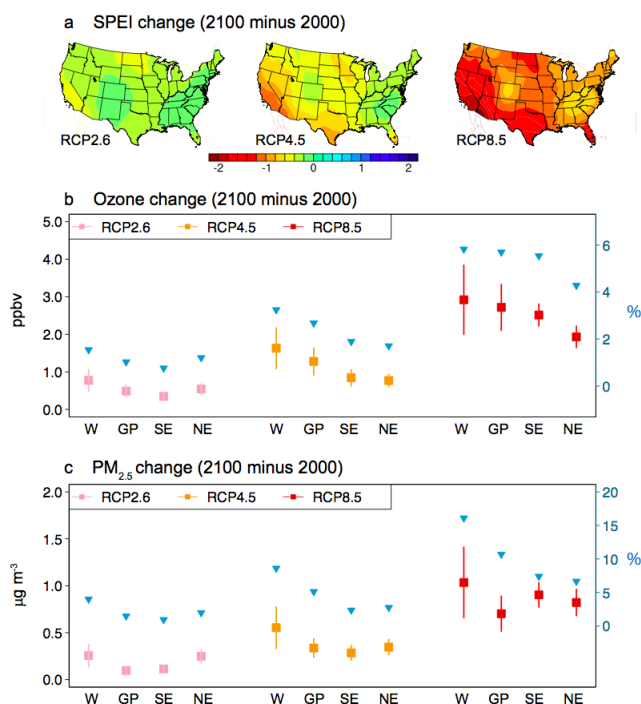


Figure 7: Predicted changes in SPEI between 2100 (2080-2099 average) and 2000 (1990-2005 average) by region under three RCP scenarios (a) from mean of four models (GISS-E2-R, GFDL-CM3, CCSM4 and MIROC-ESM-CHEM) and the estimated changes in surface ozone (b) and $PM_{2.5}$ (c) resulting from the SPEI changes alone. The four points in each RCP scenario represent the Western, Great Plains, Southeastern and Northeastern US. Error bar represents 1/2 standard deviation. Blue triangles indicate the mean percentage changes relative to the 2000 conditions (right y-axis).

10